CIRP Annals - Manufacturing Technology 62 (2013) 303–306

Contents lists available at SciVerse ScienceDirect

CIRP Annals - Manufacturing Technology

journal homepage: http://ees.elsevier.com/cirp/default.asp

A new schedule-free mandrel-less bending method for straight/pre-shaped long tubes

Takashi Kuboki [a,*], Kazuhito Takahashi [a], Kazuhiko Ono [b], Kozo Yano [b]

[a] Department of Mechanical Engineering and Intelligent Systems, University of Electro-Communications, Tokyo, Japan
[b] Komatsu Ltd., Osaka, Japan

Submitted by Manabu Kiuchi (1), Tokyo, Japan

ARTICLE INFO

Keywords:
Cold forming
Bending
Tube

ABSTRACT

The objective is to propose a new schedule-free mandrel-less draw-bending method to achieve high cross-sectional precision for straight and pre-shaped long tube, for which conventional methods lacking innovation are useless. The proposed method applies side compression on the tube. Analyses and experiments verified excellence of the method and the new method successfully reduced the error index of circularity under the severe conditions of conventional methods. The method would bring significant flexibility in manufacturing as the method is able to bend arbitrary portions of tubes and be placed in arbitrary positions of the process line.

1. Introduction

Bent tubes are used as diversified components of structures, machines, liquid and gas delivery systems [1], heat exchange tubings [2] and so on. When bent tubes are used, they need designed bending radius, circularity of cross-section, uniform or designated wall thickness, smooth outer/inner surfaces and total geometrical precision of bent portions.

This paper will present a newly developed bending method and machine that make it possible to bend arbitrary portions of long tubes, not only straight tubes but also pre-shaped or assembled shaped tubes, and obtain high precision of geometrical shape and dimension of the bent portion.

Recent machines and vehicles have been requesting precise and complex-shaped long tubes for realizing their high performance. General conventional bending methods with bending die, including mandrel or booster bending methods, cannot give solutions to the request any more. Insertion of a mandrel inside the tube during bending was once known as a proper method to improve precision [3]. However, the mandrel cannot be used for either pre-shaped or long tubes because of difficulty of insertion and positioning. Booster bending might be an alternative method [4]. However, booster bending also has difficulty, because axial compressive stress leads to wrinkle or buckling. As mandrel and booster bending methods require the tube-end portion to be straight, the flexibility of the process line is strictly limited, resulting in limited variation of the manufactured tube shape. Although a new bending method was developed to respond to these requirements by utilizing overlaid moment by 3 sets of rolls [5], the composition and controlling method are slightly complicated. Therefore, a new process has been desired which realizes cross-sectional precision for straight/pre-shaped long tubes while bending arbitrary portions in flexible order on the process line.

The authors proposed side compression bending (S.C. bending) which applies side compression for a short tube [6]. This paper presents its efficiency for straight/pre-shaped long tubes compared with booster bending, and demonstrates the application concepts to the industry. A series of finite element analyses and laboratory experiments was carried out comparing S.C. bending with booster bending with emphasis on the precision as well as three types of defects: wrinkle, buckling at clamp and buckling at straight part. The results show the excellence of the proposed method in terms of precision and forming limit in addition to significant flexibility for the order of process lines.

2. Bending methods

2.1. Side compression bending

The presented side compression bending (S.C. bending) is shown in Fig. 1. The bending die rotates, while the side compression die pushes the tube into the bending-die groove. The side compression die is composed of upper and lower dies. The upper and lower dies have slopes, which are fit to the slopes on the bending die. When the side compression die is pushed towards the bending die, the upper and lower dies clamp the tube in the vertical direction to shrink the vertical diameter d_v. Side compression δ_C, which is the total displacement of the upper and lower dies, is regulated by the spacer between the dies. Bending radius R_0 is defined at the centre axis of the tube. The tube is clamped at the position L_C, which is set to be equal to bending radius R_0.

* Corresponding author.

0007-8506/$ – see front matter © 2013 CIRP.
http://dx.doi.org/10.1016/j.cirp.2013.03.119

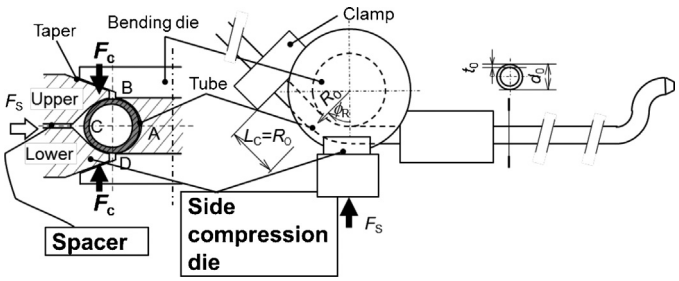

Fig. 1. Side compression bending.

As S.C. bending does not need a straight tube tail, it is applicable for pre-shaped long tubes. An example of a process which uses S.C. bending is shown in Fig. 2. In conventional methods, including mandrel or booster bending, the forming of the tube ends should be conducted after all bending processes, and the series of bending processes should be conducted from the head [H] to the tail [T] in order. On the other hand, S.C. bending is able to bend tubes in an arbitrary order, and even modify tube-bend shape after total assembly as seen in Fig. 2(e). The processing of tube ends or other parts is able to be placed at arbitrary positions of the process line, at the beginning of the line for example. As a result, S.C. bending gives flexibility to process design that would realize the most suitable, intelligent and the most productive manufacturing.

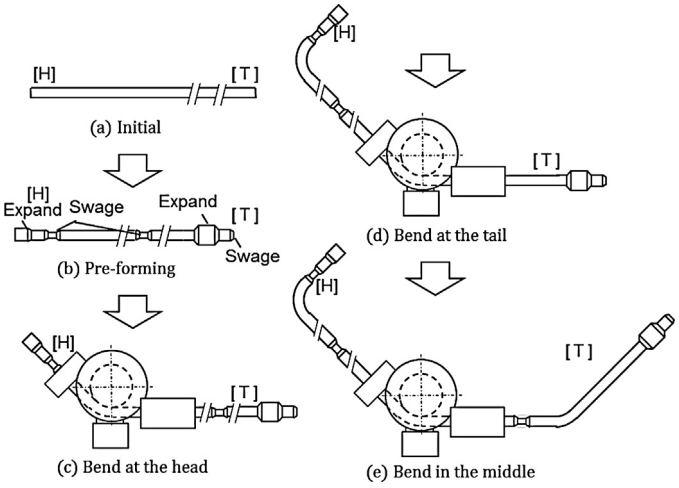

Fig. 2. Application of S.C. bending in process line. (a) Initial, (b) pre-forming, (c) bend at the head, (d) bend at the tail, and (e) bend in the middle.

An experimental example of tube cross sections obtained by S.C. bending is shown in Fig. 3. When side compression δ_C was 0 mm, the tube wall of extrados [C] moved towards the centre of the tube and extrados [B–C–D] flattened. The error index of circularity was evaluated by flatness, defined by the following equation:

$$D_F = \frac{d_v - d_H}{d_0} \quad (1)$$

where d_v and d_h are diameters in vertical and horizontal directions, respectively.

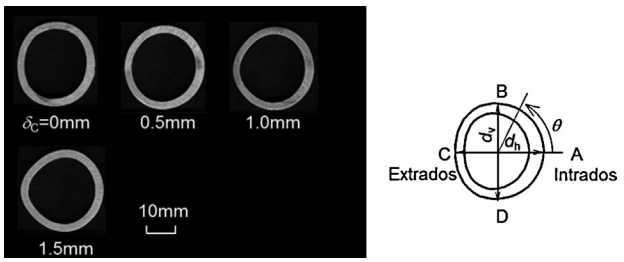

Fig. 3. Effect of side compression bending on circularity (5056 aluminium alloy, thickness t_0 = 3.2 mm, radius ratio R_0/d_0 = 3).

The vertical diameter d_v decreased with increase of side compression δ_C. As the peripheral length was not affected by δ_C, the horizontal diameter d_h expanded, resulting in improvement of circularity. Excessive δ_C led to over-expansion of d_v at δ_C = 1.5 mm.

2.2. Booster bending

The efficiency of S.C bending was compared to booster bending, which is one of the conventional methods and is schematically shown in Fig. 4. The axial compressive stress σ_a should be imposed for improvement of circularity of the tube. However, axial compressive stress often causes defects as shown in Fig. 5. Wrinkle generally tends to occur at the intrados when bending radius is small. Axial compressive stress would increase this tendency. When the axial compressive stress is too large, buckling phenomena would be observed at [P] and [Q] as shown in Fig. 5(b). The excessive axial compressive stress would cause buckling at clamp [P], followed by secondary buckling at [Q]. Furthermore, if the tube is long, buckling would occur at the straight part as shown in Fig. 5(c).

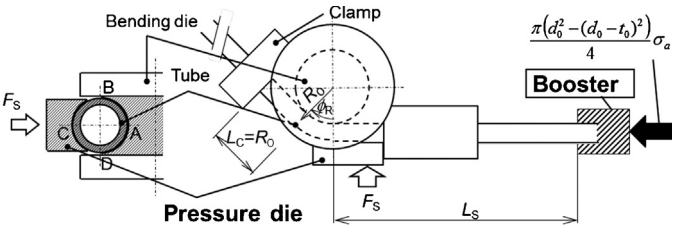

Fig. 4. Booster bending.

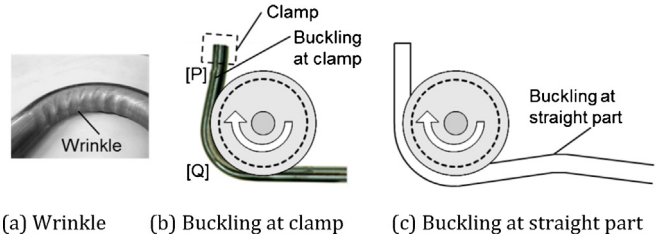

Fig. 5. Defect in booster bending. (a) Wrinkle, (b) buckling at clamp, and (c) buckling at straight part.

On the other hand, S.C. bending does not need any axial compressive stress, which causes or propels defects. In order to verify the excellence of S.C. bending a series of analyses and experiments were carried out. Table 1 shows the details of tubes for bending and Table 2 shows bending condition. Carbon steel for general structural purposes STK 490 (JIS) was used.

Table 1
Specimen for tube bending.

Material		Medium carbon steel STK490 (JIS)
	Tensile strength σ_B/MPa	490
	Hardening exponent n	0.15
	Yield stress σ_y/MPa	327
Dimension	Outer diameter d_0/mm	27.2
	Thickness t_0/mm	2.0–3.2

Table 2
Bending conditions.

Common	Bending radius R_0/mm	$1.5\,d_0$–$3.0\,d_0$
	Rotate angle ϕ_R/mm	90
	Pressure force F_S/kN	30 in experiment Pressure die position was fixed in FEM
Side compression bending	Side compressive displacement δ_c/mm	0–2.0
Booster bending	Axial compressive ratio σ_a/σ_B	0–40%

3. Evaluation by numerical method

As experiments might include some disturbance, numerical analyses were conducted to evaluate S.C bending and booster bending under disturbance-less condition. Elastic-plastic analysis was carried out using the commercial code ELFEN, which was developed by Rockfield Software Limited, Swansea [7]. A von Mises' yield criterion was adopted, and the normality principle was applied to the flow rule. Constraints were dealt with by the penalty function method. A dynamic explicit scheme was used for evaluating defects with shortening the calculation time in the three-dimensional model. A static implicit scheme was not applicable for defect evaluation because it stopped at the beginning of buckling and failed to show the buckling phenomena. Hexahedral elements were adopted and the model is shown in Fig. 6.

As fewer wrinkles were observed in numerical bending than in experimental bending, some index was needed for wrinkle evaluation. Hereby, the axial strain at extrados ε_{ax} was simply taken as an index for evaluation of wrinkle. The critical value of ε_{ax} for wrinkle was determined as 0.25 by comparing numerical and experimental results.

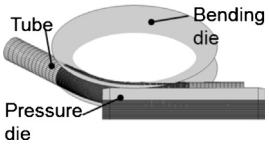

Fig. 6. Model in FEM.

Fig. 7 shows buckling at clamp observed in the numerical bending. Increase of axial compressive stress σ_a and bending radius R_0 led to buckling, while influence of thickness on buckling phenomena was small. When compressive stress ratio σ_a/σ_B was 30% for the radius ratio R_0/d_0 of 3.0, the tube started to deflect from the bending die as shown in Fig. 7(b) and (c). When σ_a/σ_B was 40% and R_0/d_0 was 3.0, buckling appeared clearly. However, when R_0/d_0 was 1.5, no buckling appeared.

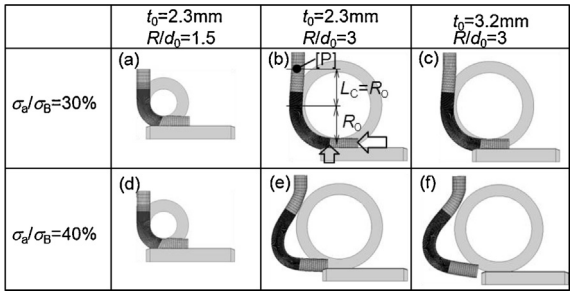

Fig. 7. Buckling at clamp in FEM.

In the numerical model, tube length was selected satisfactorily short so as not to make buckling at the straight part. Instead, buckling at the straight part was evaluated by Euler's equation as follows [8]:

$$P = \frac{2\pi^2 EI}{L_S^2}, \tag{2}$$

assuming the bending point would be pinned and that the boosted end would be built-in.

4. Effect of side compression bending

Results on defects in the finite element method and experiments are shown in Table 3. Using criteria of strain $\varepsilon_{ax} > 0.25$ mm might be simple but appropriate for prediction of wrinkle, as the numerical and experimental results were in good agreement. As no

Table 3
Defects in booster bending predicted by FEM ($t_0 = 2.3$ mm).

		Bending radius ratio R_0/d_0							
		1.5		2.0		2.5		3.0	
		FEM	Exp	FEM	Exp	FEM	Exp	FEM	Exp
Side compressive displacement δ_C/mm	0	S	S	S	S	S	S	S	S
	0.5	S	S	S	S	S	S	S	S
	1.0	S	S	S	S	S	S	S	S
	1.5	S	S	S	S	S	S	S	S
	2.0	S	S	S	S	S	S	S	S
Axial compressive ratio σ_a/σ_B (%)	0	S	S	S	S	S	S	S	S
	10	W	W	S	S	S	S	S	S
	20	W	–	S	S	S	S	S	S
	30	W	–	W	W	S	S	S	S
	40	W	–	W	–	W Bc	Bc	Bc	Bc

S, success (no defects); W, wrinkle; Bc, buckling at clamp; –, not tried.
Wrinkle is evaluated by criterion of axial strain at intrados $\varepsilon_{ax} > 0.25$.

axial compressive stress was applied in S.C. bending, neither buckling nor wrinkle was observed.

On the other hand, in booster bending, wrinkle tends to appear with smaller axial compressive ratio σ_a/σ_B with decrease of bending radius. Buckling was a dominant factor which determined the applicable axial compressive stress σ_a for larger bending ratio of $R_0/d_0 > 2.5$ resulting in little improvement of circularity.

Furthermore, flatness was evaluated in the numerical analyses. The numerical results for S.C. bending are shown in Fig. 8. It is noteworthy that flatness D_F becomes zero at optimum δ_C regardless of thickness t_0 when bending radius ratio $R_0/d_0 = 3.0$ in Fig. 8(a). In other words, if the appropriate side compression δ_C is selected, flatness D_F could be reduced to zero.

When the thickness t_0 was 3.2 mm in Fig. 8(b), the effect of side compression δ_C was significantly affected by bending radius ratio R_0/d_0. When R_0/d_0 was larger than 2.0, the effect of S.C. bending for improvement of circularity was significant.

The result for booster bending is shown in Fig. 9 for comparison. As bending radius ratio R_0/d_0 was large at 3.0 and thickness t_0 was thick at 2.3 mm, the bending condition was the mildest. The circularity was not improved very much even under the mildest condition. Flatness decreased with increase of axial compressive ratio σ_a/σ_B up to 20%. However, further increase of σ_a/σ_B led to

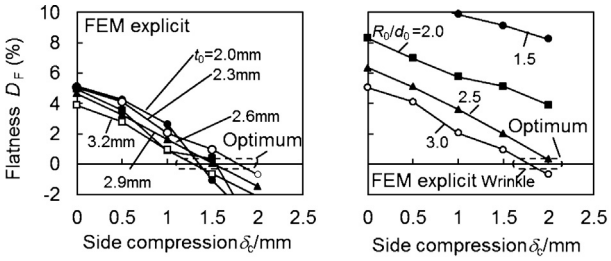

(a) For different thickness (Bending radius R_0/d_0=3.0) (b) For different bending radius (Thickness t_0=3.2 mm)

Fig. 8. Improvement of circularity by side compression bending in FEM (length of straight part $L_S < 1$ m). (a) For different thickness (bending radius $R_0/d_0 = 3.0$) and (b) for different bending radius (thickness $t_0 = 3.2$ mm).

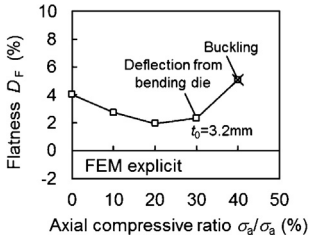

Fig. 9. Circularity change by booster bending in FEM (bending radius $R_0/d_0 = 3.0$, thickness $t_0 = 3.2$ mm, length of straight part $L_S < 1$ m)).

deflection of the tube from the die groove as shown in Fig. 7(b) and (c), and buckling as shown in Fig. 7(e) and (f), making tube circularity deteriorate.

5. Discussion

5.1. Improvement of circularity in analyses and experiments

The effect of side compression bending and booster bending for improvement of circularity was compared in analyses and experiments for wall thickness t_0 = 2.3 mm. The results are shown in Fig. 10.

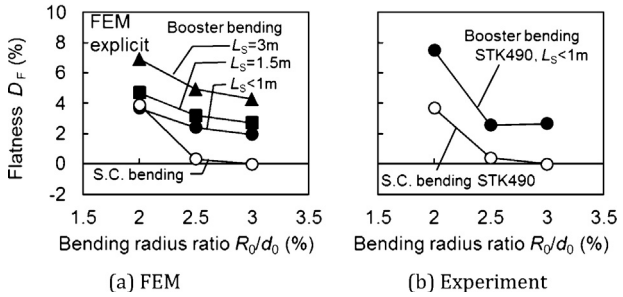

(a) FEM (b) Experiment

Fig. 10. Flatness at optimum conditions for booster bending and side compression bending (t_0 = 3.2 mm). (a) FEM and (b) experiment.

Side compression bending showed excellent performance and realized almost zero flatness for t_0 = 2.3 mm when R_0/d_0 was larger than 2.0, if an appropriate side compression δ_C was selected. On the other hand, as booster bending with excessive axial compressive ratio led to buckling at the clamp, flatness D_F was over 2% even at the optimum conditions.

Furthermore, buckling at the straight part of Fig. 5(c) was considered by Euler's equation (2) for straight-part length L_S of 1.5 and 3 m in booster bending. As the limit axial compressive stress was calculated by Eq. (2), the minimum flatness was able to be evaluated using a diagram like Fig. 9 by interpolation. The results are added in Fig. 10. When the tube-straight part L_S was less than 1 m, no buckling was predicted at the straight part. However, when L_S was larger than 1 m, the effect of booster bending was predicted to be small as the axial compressive stress should be limited for prevention of buckling at the straight part.

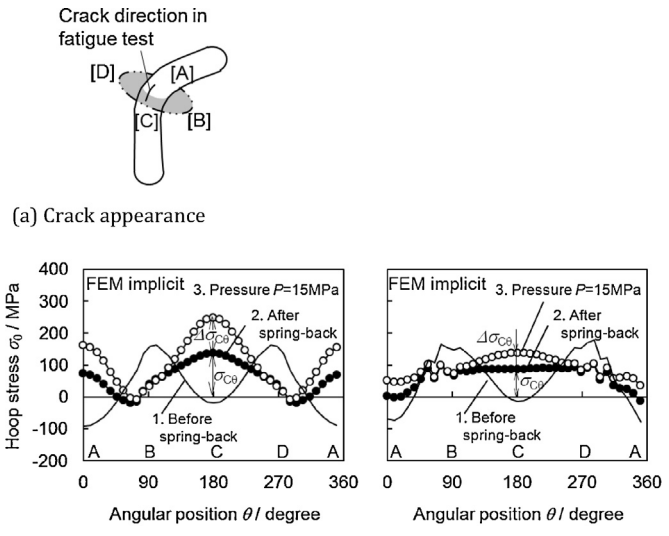

(a) Crack appearance

(b) Booster bending (L_S<1m) Flatness D_F = 2.46 %, σ_a/σ_B =20%

(c) Side compression bending Flatness D_F = 1.48 %, δ_C =0.10mm

Fig. 11. Hoop stress at the centre of bending arc in FEM (d_0 = 3.2 mm, R_0/d_0 = 3.0). (a) Crack appearance, (b) booster bending ($Ls < 1$ m), flatness D_F = 2.46%, σ_a/σ_b = 20%, (c) side compression bending, flatness D_F = 1.48%, δ_c = 0.10 mm.

5.2. Stress change in operation of construction machines

When bent tubes are used in construction machines, the tubes are subjected to repeated internal pressure. The stress change on the tube surface under internal pressure was evaluated by FEM. The implicit scheme was adopted for more precise evaluation for stress. As the crack line was generally observed in the vertical direction to hoop direction under repeated internal pressure at position [C] in Fig. 11(a), hoop stress was evaluated. The results are shown in Fig. 11(b) and (c).

While hoop stress was high at the side points [B] and [D] during bending before spring-back, it was high at the extrados [C] after spring-back and was higher under pressure P of 15 MPa. [C] was the place where crack appeared in the fatigue test. Side compression bending has a significant effect of suppression of hoop stress, compared to booster bending. Both of the stresses at [C] after spring-back $\sigma_{C\theta}$ and under internal pressure $\Delta\sigma_{C\theta}$ in S.C. bending are much less than those in booster bending. $\sigma_{C\theta}$ was reduced by 40% and $\Delta\sigma_{C\theta}$ was reduced by 50%.

6. Conclusions

This paper presented a newly developed bending method, side compression bending (S.C. bending), that makes it possible to bend arbitrary portions of not only straight long tubes but also pre-shaped long tubes, and obtain high precision of the geometrical shape and dimension of the bent portion. Conventional methods, including mandrel or booster bending, were never applicable for such kinds of usage. A series of numerical analyses and experiments was conducted for examination of the efficiency of S.C. bending with emphasis on the defects and circularity. The results showed that S.C. bending was efficient to improve the circularity much more than booster bending even for short tubes, in particular, when the bending radius was relatively large around 2.5–3 times of tube diameter, under which conditions booster bending would cause buckling at the clamp. The advantage was much greater for tubes with length longer than 1 m under which conditions booster bending would cause buckling at the straight part.

The proposed S.C. bending would be useful for the manufacturing of straight or pre-shaped long tubes, which are used in construction machines, for example. Side compression bending would be efficient when both ends are previously deformed, bent, swaged or sealed, and mandrels and booster cannot be applied. Therefore, the proposed method would bring significant flexibility in manufacturing as the process designers are able to place tube bending at arbitrary positions of the process line, with fabricating a bent portion with high precision at arbitrary positions of tubes. Side compression bending is excellent in both improvement of circularity, manufacturing complex shaped long tube, and giving flexibility to process scheduling.

References

[1] Hayashi C (2000) *Advancement in Tube Making Technology and Engineering. For the Final Renaissance of Tube Making Technology*, ISIJ. pp. 17–57 (in Japanese).
[2] Kuboki T, Furugen M, Osaka S, Ono T (1998) Development of Die-Less Bending Process for Precision U-Bent Tube. The 7th International Conference on Steel Rolling. *Chiba* 981–987.
[3] Utsumi N, Sakaki S (2002) Countermeasures Against Undesirable Phenomena in the Draw-Bending Process for Extruded Square Tubes. *Journal of Materials Processing Technology* 123(2):264–269.
[4] Aizu S (1966) Tube Special Bending by Pipe Bender. *Technology of Press* 4–8:75–80. (in Japanese).
[5] Hermes M, Chatti S, Weinrich A, Tekkaya A (2008) Three-Dimensional Bending of Profiles with Stress Superposition. *International Journal of Material Forming* 1(1):133–136.
[6] Takahashi K (2012) Suppression of Flatness in Circular Tube-Draw Bending by Applying Side Compression. *Material Transactions* 53(5):870–874.
[7] de Souza Neto EA, Peric D, Dutko M, Owen DRJ (1996) Design of Simple Low Order Finite Elements for Large Strain Analysis of Nearly Incompressible Solids. *International Journal of Solids and Structures* 33(20–22):3277–3296.
[8] Timoschenko SP, Young DH (1968) *Elements of Strength of Materials*, Maruzen as Asian edition. pp. 268–273.